

Overview of ASDEX Upgrade results

Arne Kallenbach on behalf of the ASDEX Upgrade team and the EUROfusion MST1 team*

Max-Planck-Institute for Plasma Physics
D-85748 Garching

*see appendix of H. Meyer et al., (OV/P-12) Proc. 26th IAEA Fusion Energy Conf., Kyoto, Japan

the 2014-2016 AUG programme is a joint venture of IPP and EUROfusion

CN-234 OV/2-1



This work has been carried out within the framework of the EUROfusion Consortium and has received funding from the Euratom research and training programme 2014-2018 under grant agreement No 633053. The views and opinions expressed herein do not necessarily reflect those of the European Commission.

- Recent hardware upgrades
- Non-inductive operation
- ELM suppression with magnetic perturbations
- Pedestal stability and confinement
- Power exhaust
- Scenario integration and extrapolation to large devices

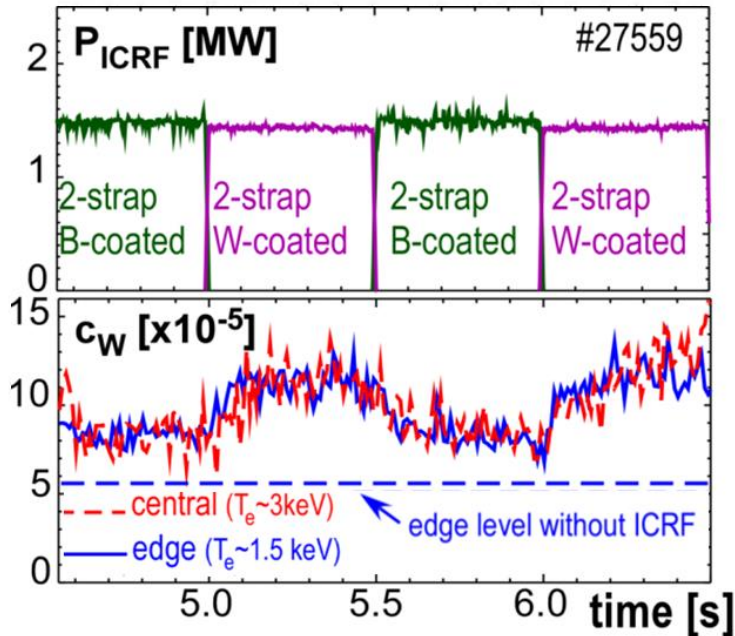
Special emphasis is placed on the presence of tungsten (W) plasma facing components

for ELM heat load studies and integrated edge/wall solutions see: **H. Meyer OV/P-12** later today
for disruption physics, mitigation and runaways, see **Martin EX/P6-23, Papp EX/9-4, Pautasso EX/P6-38**
Plyusnin EX/P6-33

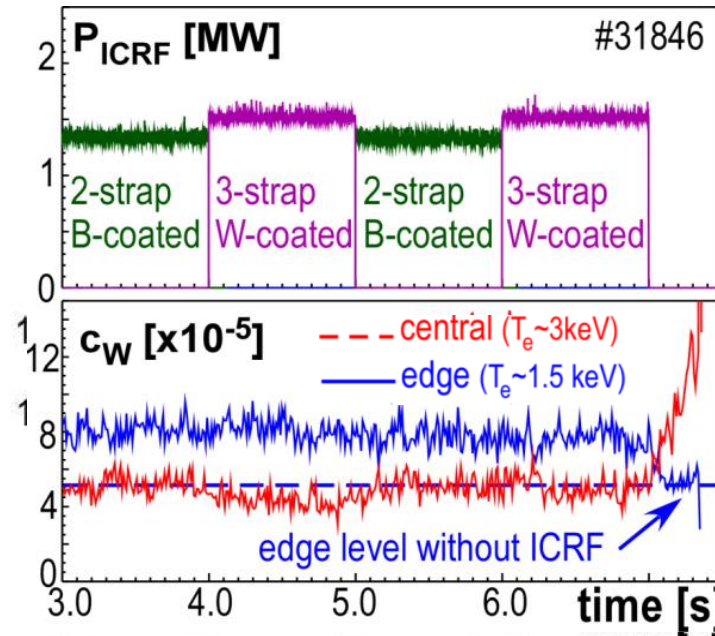
New 3-strap ICRF antenna pair for reduced W release

- performs as predicted, factor 2 reduced W release as for 2-strap antenna with B limiters

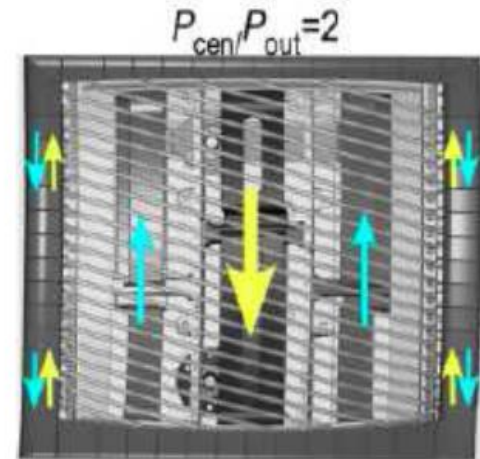
2-strap antenna



new 3-strap antenna



compensation of image currents in antenna frame

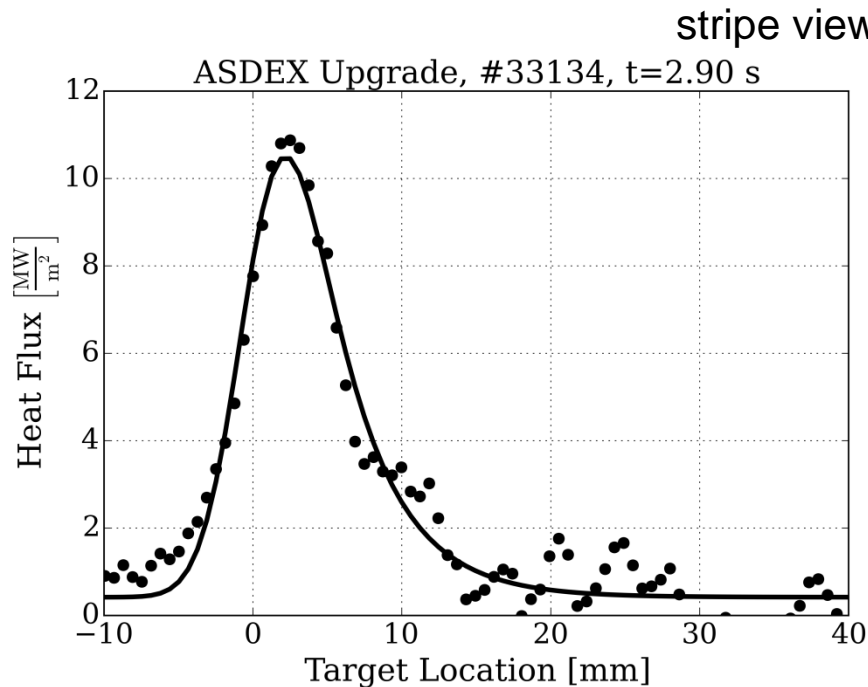


the success of the 3-strap antennas and its model validation paves the way for future ICRF in DEMO

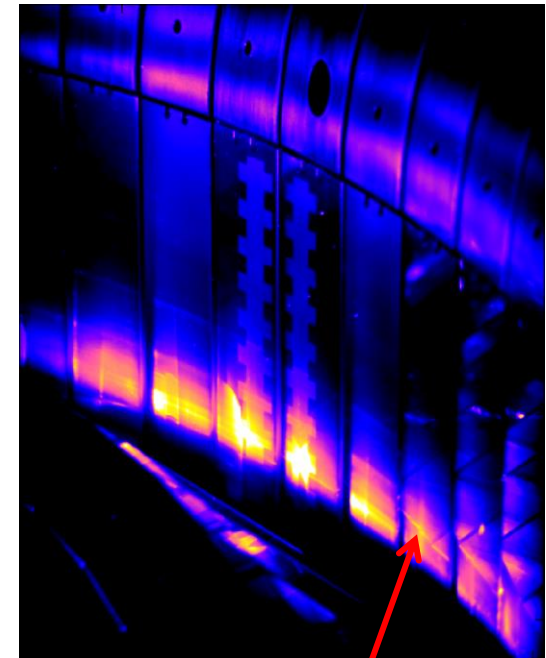
J.M Noterdaeme, EX/P6-26, Thu

Massive tungsten divertor performed well in operation

more than 10 MW/m² inter ELM peak load for 5 s measured by IR in low density, medium power H-mode



full IR view (33303, less power, more gas)



more on IR and heat flux:

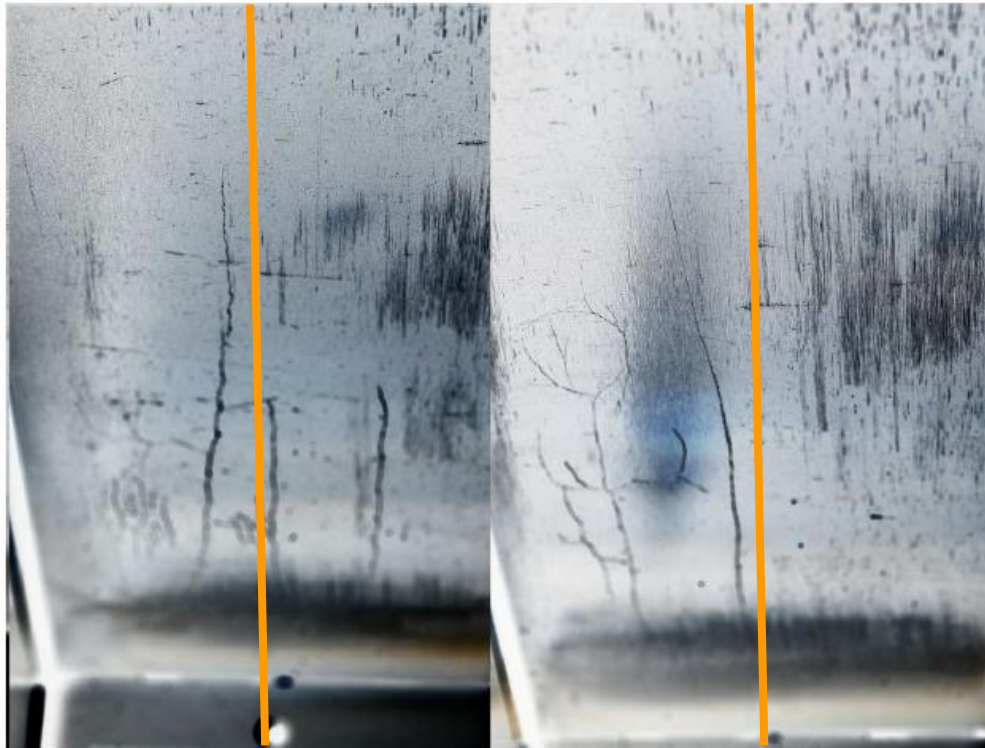
B. Sieglin, EX/7-3R, Fri

H. Meyer, OV/P12 Mon

reliable divertor operation (apart from some Langmuir probe melting), but cracks observed

Cracks formed – through tile and at the surface

- cracks not observed in high heat flux tests in GLADIS before
- forces during disruption in addition to thermo-mechanical stresses



A. Herrmann, PSI 2016

PWI (mainly He)

A. Hakola, EX/P6-22 Thu

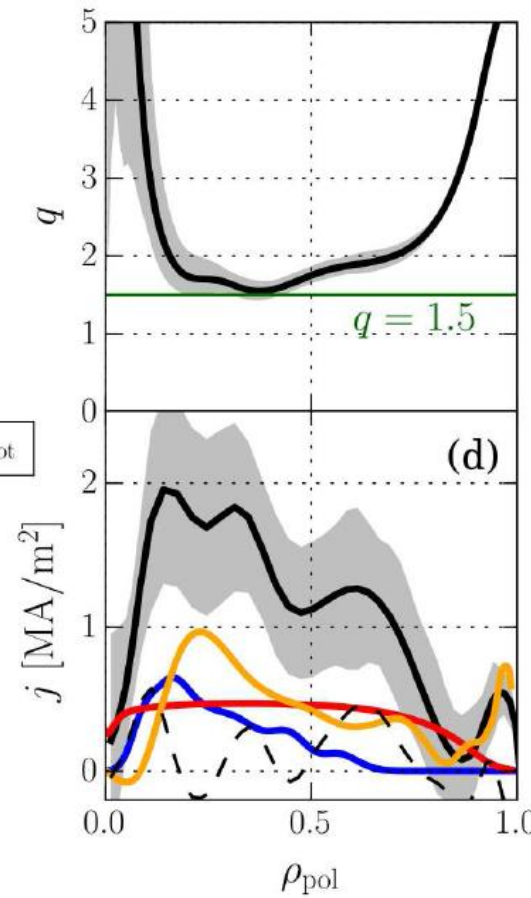
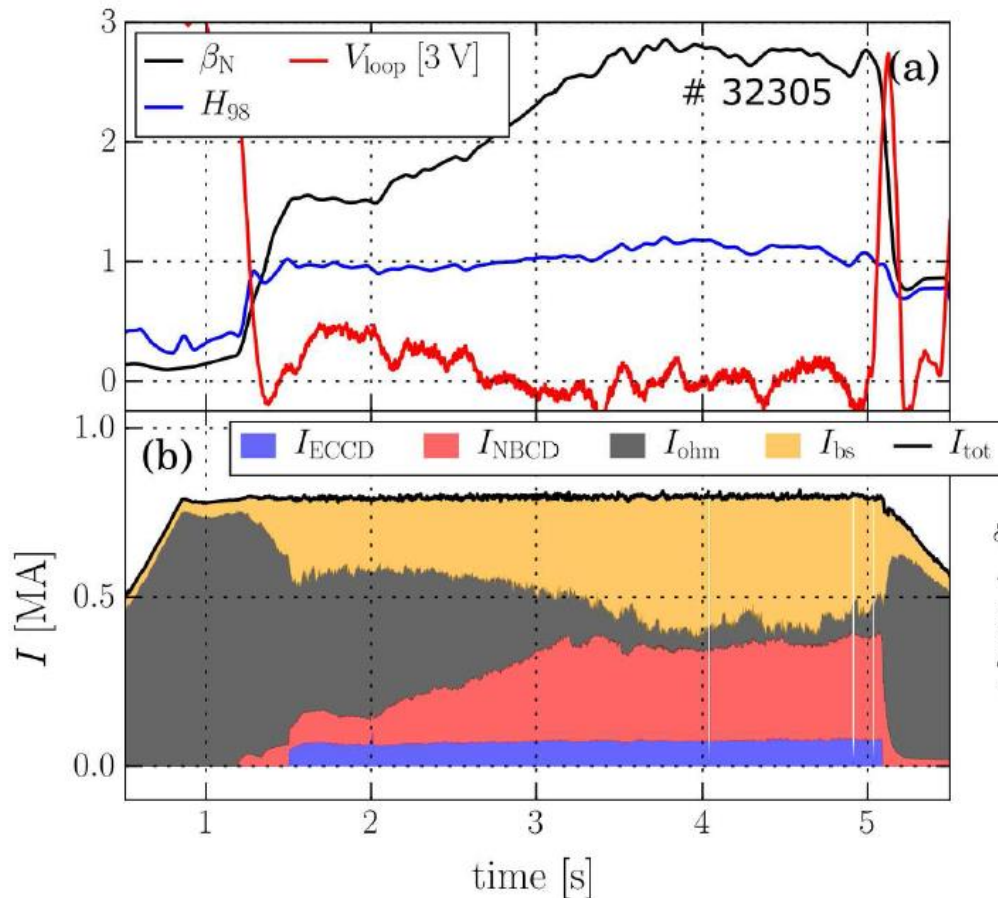
FEM calculations suggest vertical tile splitting for crack avoidance (done in current AUG vent)
¼ of tiles will be made from more ductile material 97 % W, 2 % Ni, 1 % Fe (magnetic)

Scenario development

- Non-inductive operation
- ELM suppression

Fully non-inductive operation at $I_p = 0.8$ MA

- about 40 % of I_p driven by NBCD (11 MW NBI), 50 % bootstrap, 10 % ECCD (2.7 MW)
- ECCD used to tailor current profile for optimum stability and $q_{\min} > 1.5$



- fresh boronization

J.Stober, PostDeadline, Sat.

NBCD:
C. Hopf, EX/P6-28, Thu

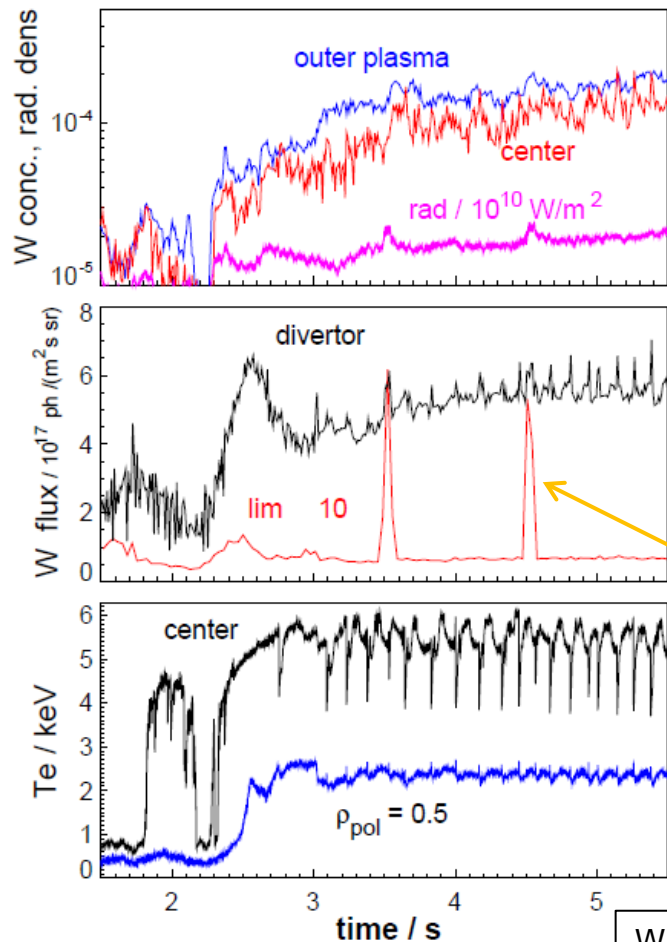
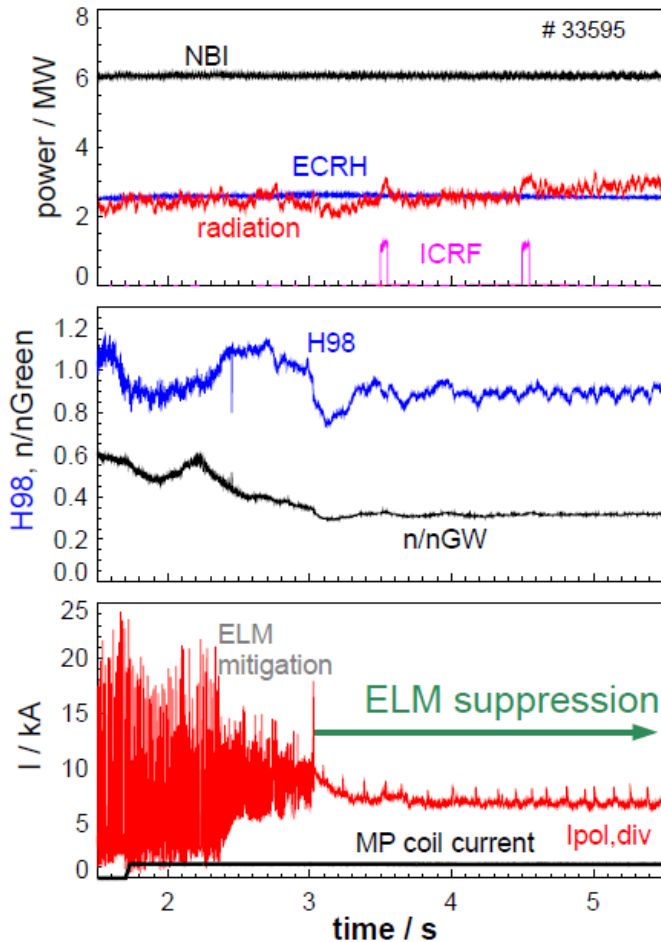
improved diagnostics: MSE, IMSE, polarimetry

MHD at high β :

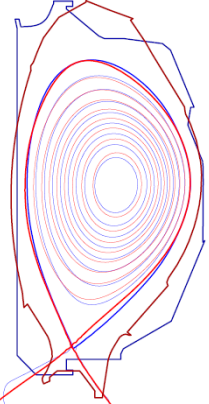
V. Igochine, EX/P6-24, Thu

ELM suppression by RMPs obtained, finally

- full ELM suppression obtained in AUG. trick: δ -dependence of threshold as found in DIII-D
- no accumulation of W at pedestal top



DIII-D 164362
 AUG 33133
 (minor radius $a \times 1.19$)



quite high W conc.
 due to hot divertor

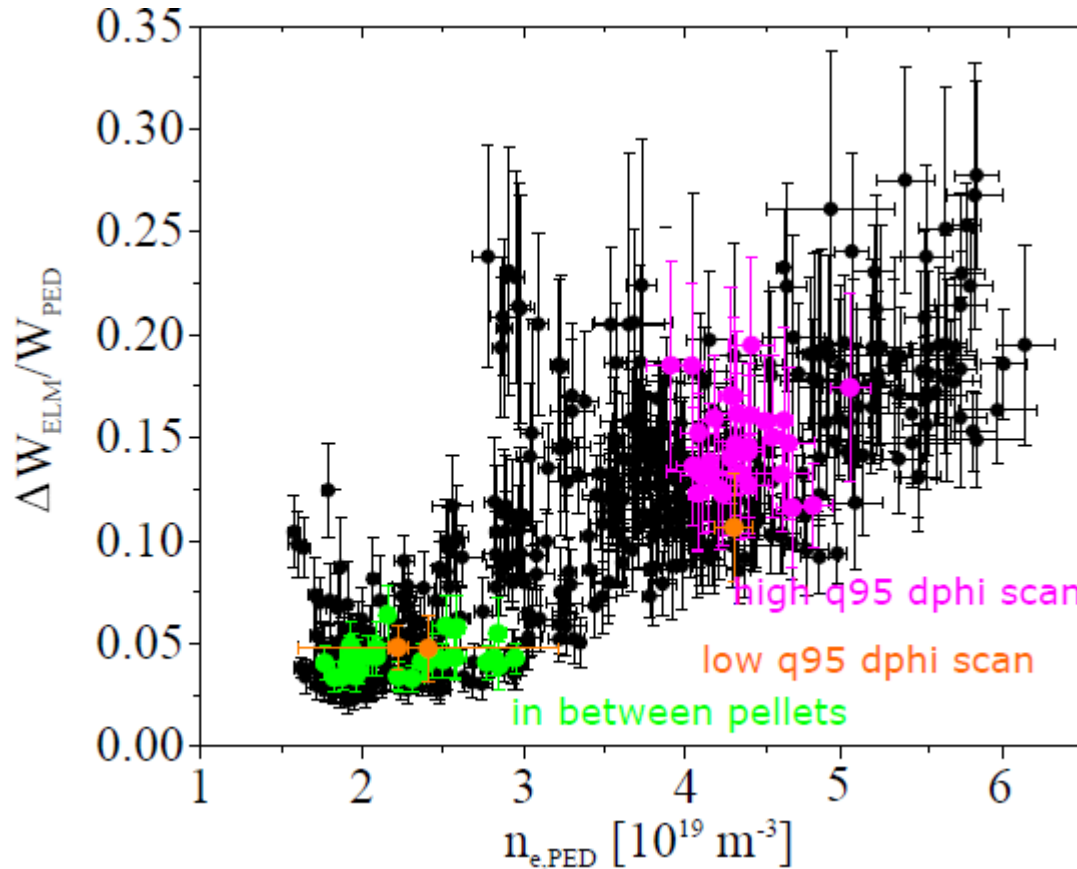
W blips from midplane limiter
 (ICRF detuned phasing)
 exhibit normal decay times

scenario can only be reached with prior ELM mitigation and fresh boronization

W. Suttrop, EPS 2016, R. Nazikian, PD, Sat

Relative ELM size depends mainly on pedestal density w/wo MPs

- ELM mitigation closely connected to density pump-out



N. Leuthold, subm. PPCF

low collisionality $\nu_{ped}^* < 1$

edge plasma response to MPs:

M. Willensdorfer, EX/P6-25 Thu

non-linear JOREK modelling:

F. Orain, TH/P1-26, Tue

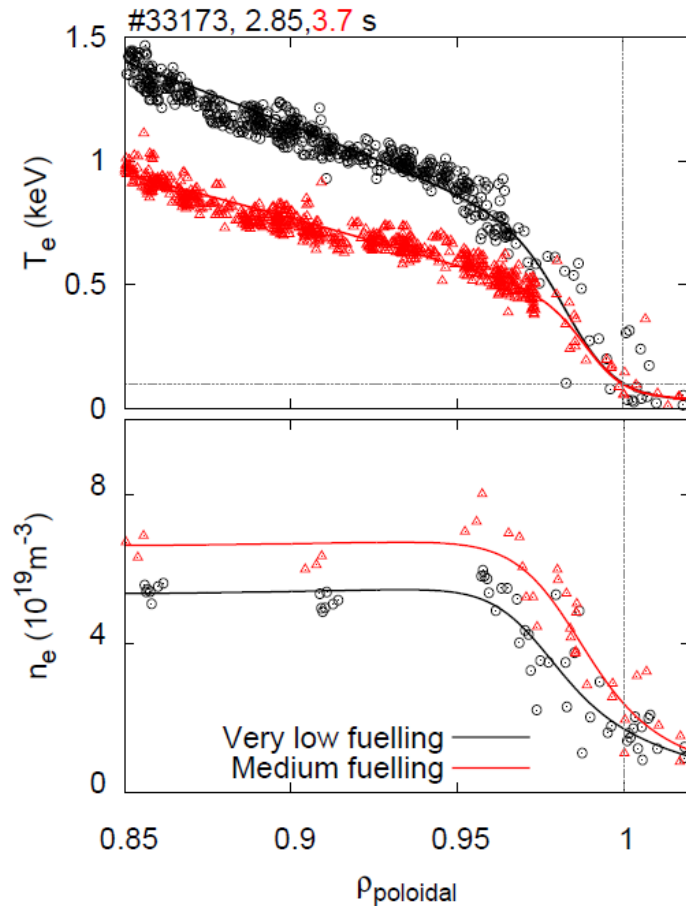
fast ion losses with MP:

M. Garcia-Munoz, EX/6-1, Thu

$n_{e,ped}$ gives better correlation compared to ν^* or pedestal pressure

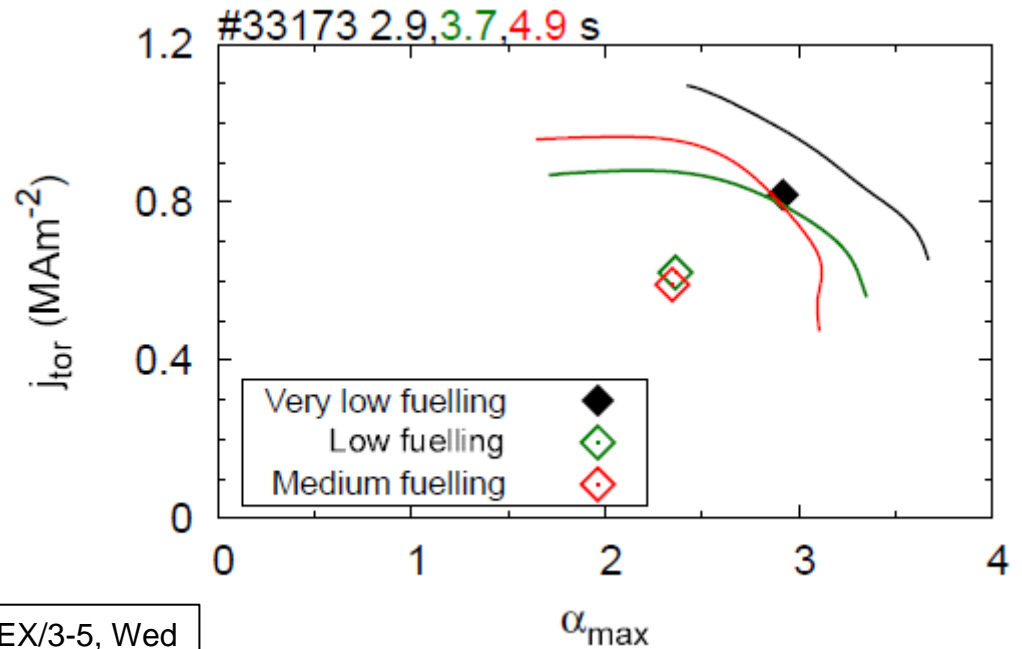
Pedestal physics

- D fueling shifts density profile outward – T profile anchored at separatrix



Stability analysis:

- unfavourable alignment of shear and max. pressure gradient

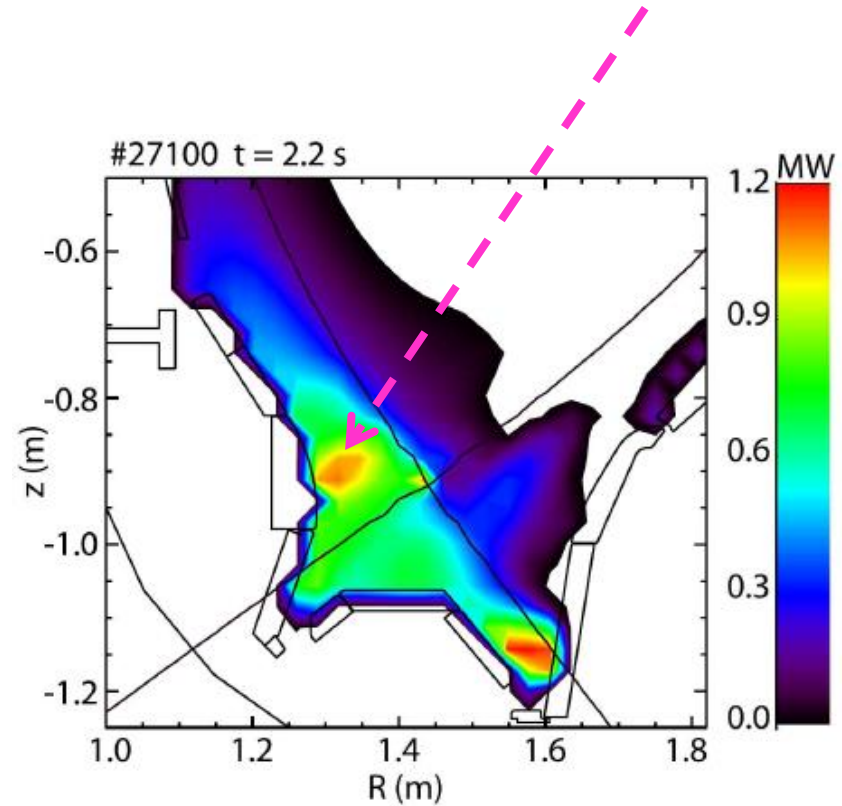
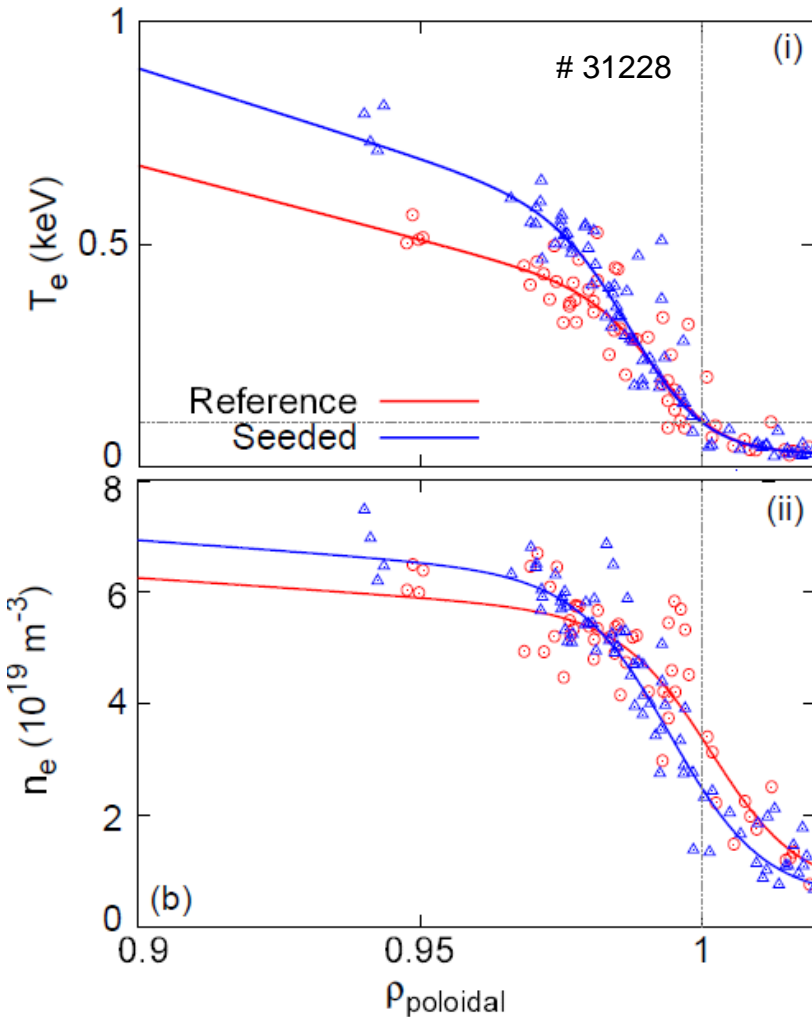


recall $\alpha \propto q^2 dp/dr$

M. Dunne, EX/3-5, Wed

Effect of N seeding via HFSHD as heating power reduction

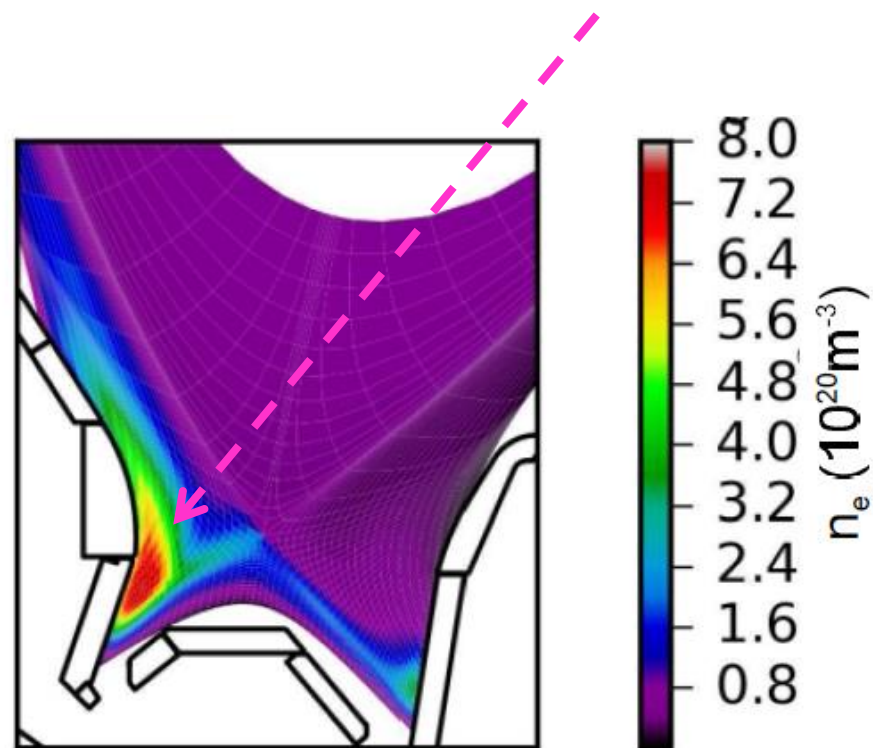
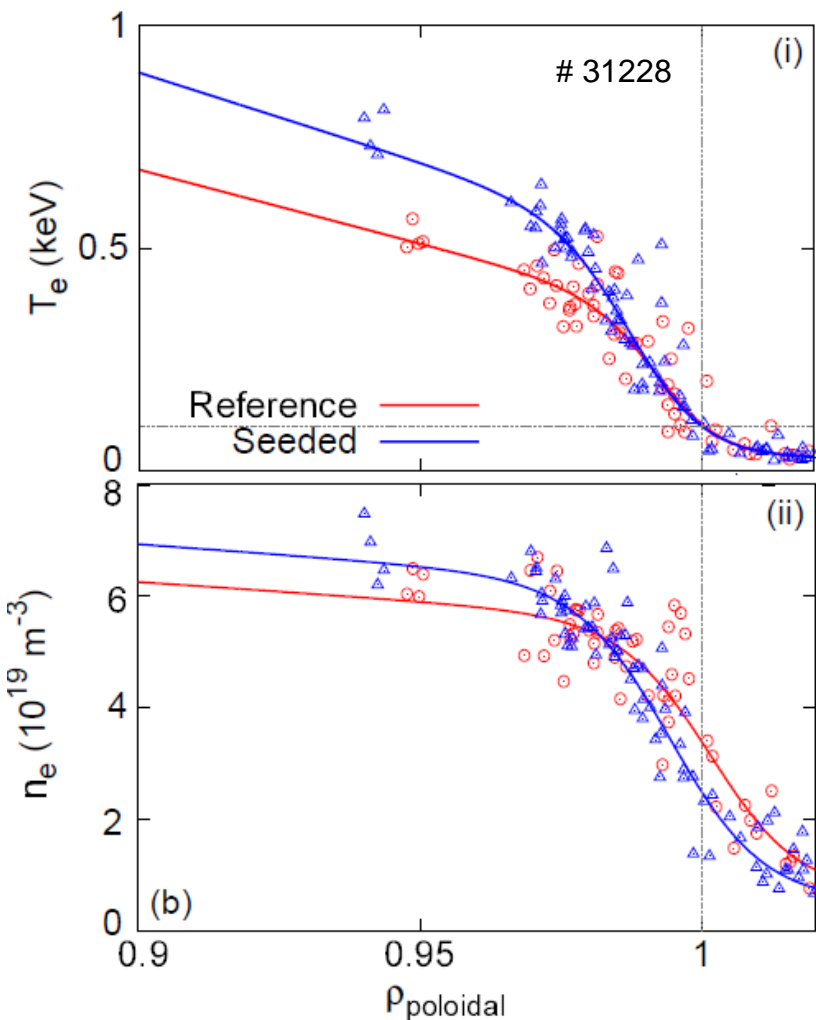
- N seeding effects fueling via reduction of high field side high density (HFSHD)



HFSHD modelling: F. Reimold, EXS/P6-191, Thu

Effect of N seeding via HFSHD as heating power reduction

- N seeding effects fueling via reduction of high field side high density (HFSHD)



effect of HFSHD
meanwhile reproduced with SOLPS modelling

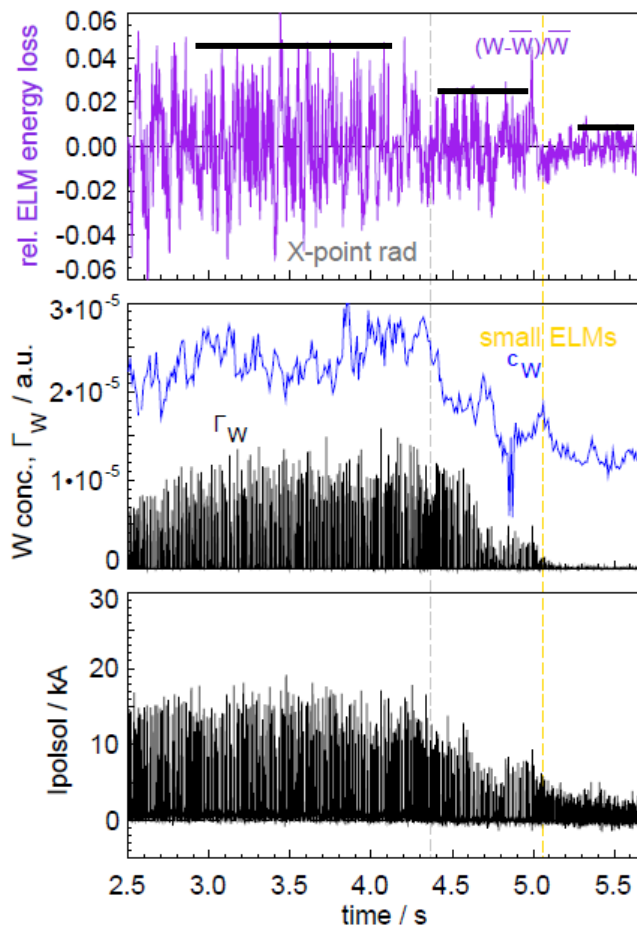
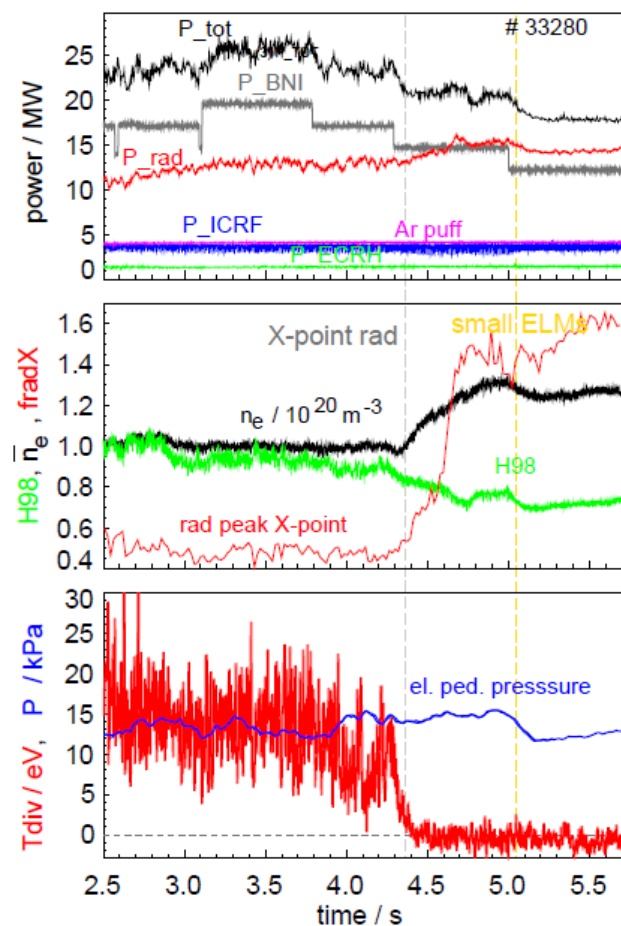
HFSHD modelling: F. Reimold, EXS/P6-191, Thu

Power exhaust

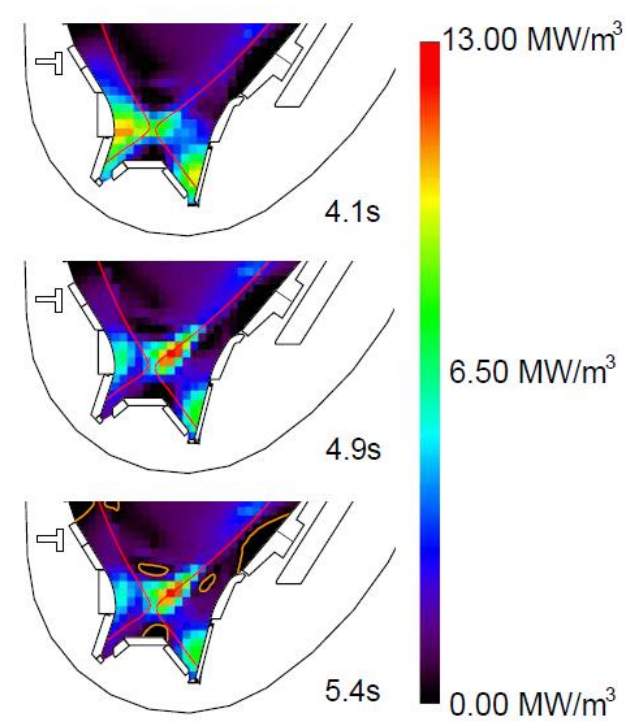
- X-point radiator
- Integration with pellet fueling
- Divertor impurity enrichment

Detachment studies with X-point radiator

- X-point radiator at pronounced detachment with N and Ar seeding
- favourable properties: cold divertor with low power load, no W sputtering, smaller ELMs
- expected to be feedback-controllable

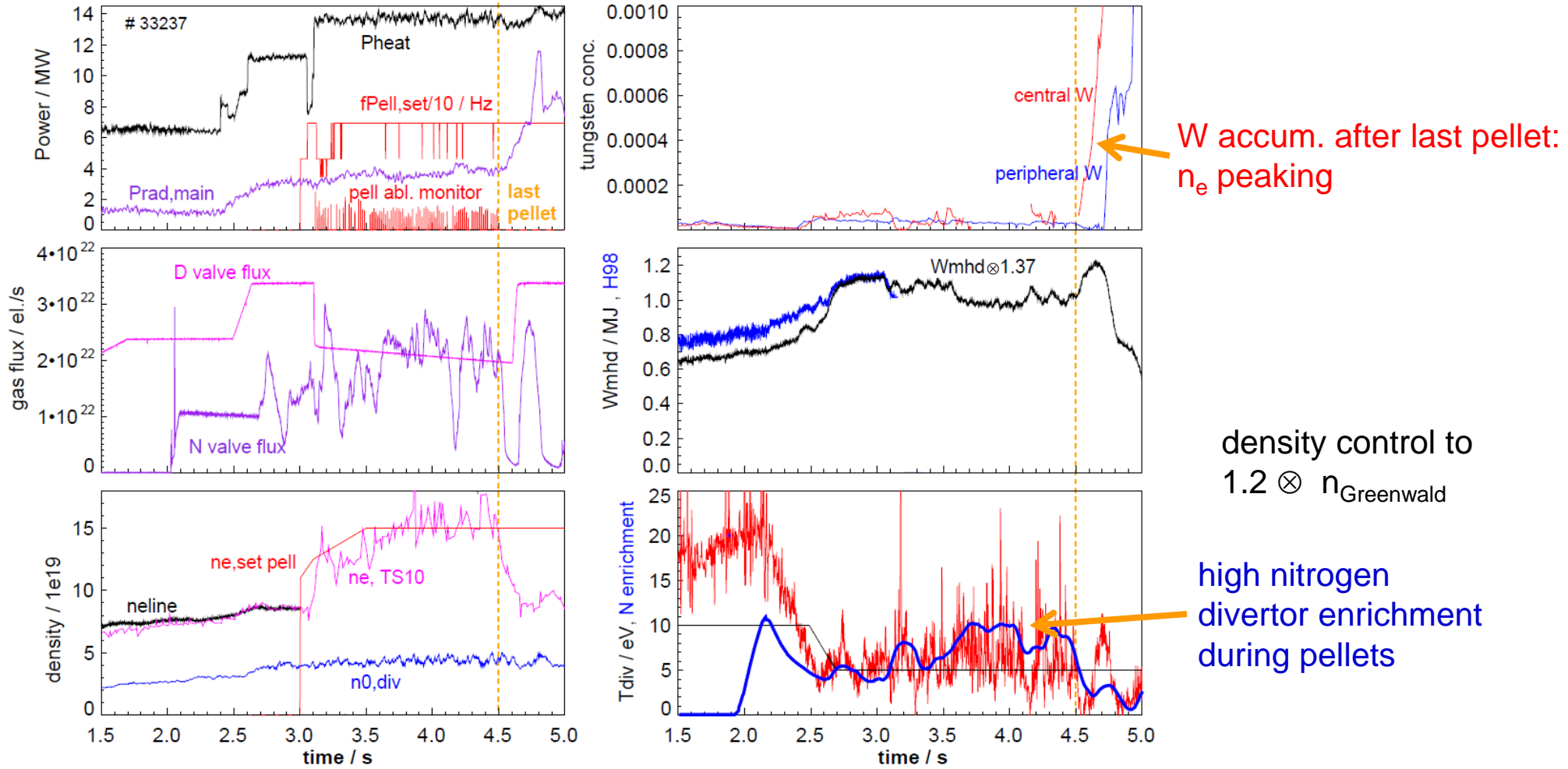


M. Bernert, PSI 2016



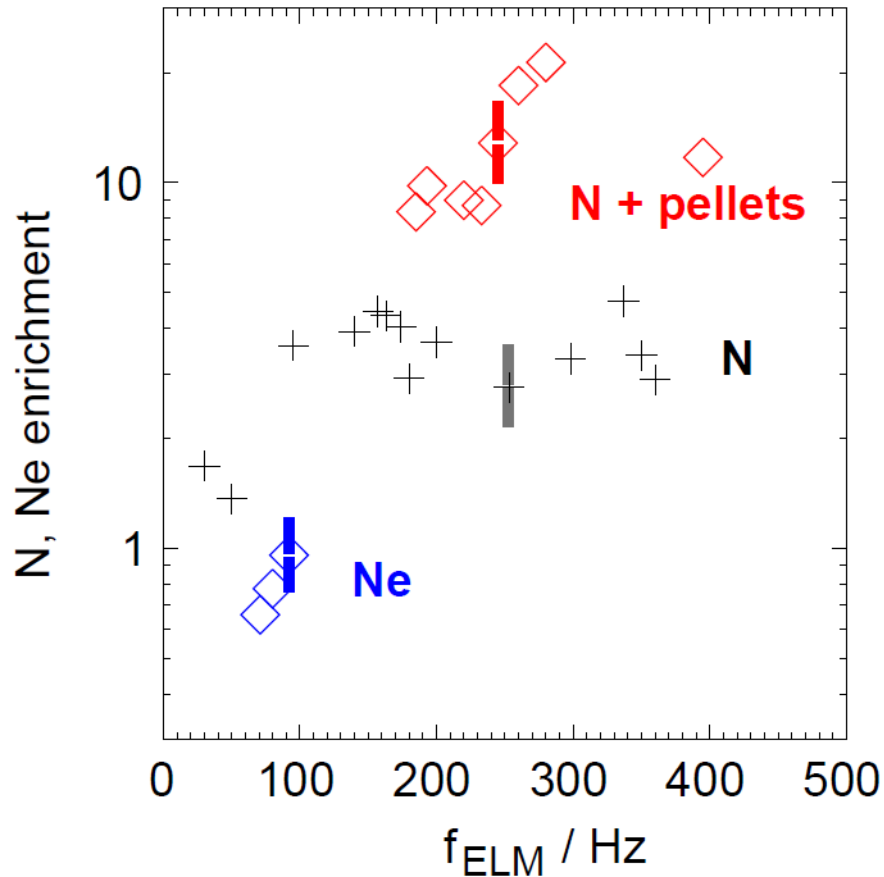
more: M. Wischmeier, PD, Sat

Integration of Tdiv feedback control and pellet density control



impurity divertor enrichment

$$E = \frac{\Gamma_Z}{Z \Gamma_D} / \frac{n_Z}{n_e}$$



ELMs enhance E via impurity flushing, reducing $c_{Z,core}$

other effects:

- impurity ionization length
- neoclassical pedestal inward drift

N, Ne enrichment modelling: F. Reimold, EXS/P6-191, Thu

a high divertor enrichent E is key for efficient power exhaust with low core impurity content

Challenges caused by tungsten PFCs.

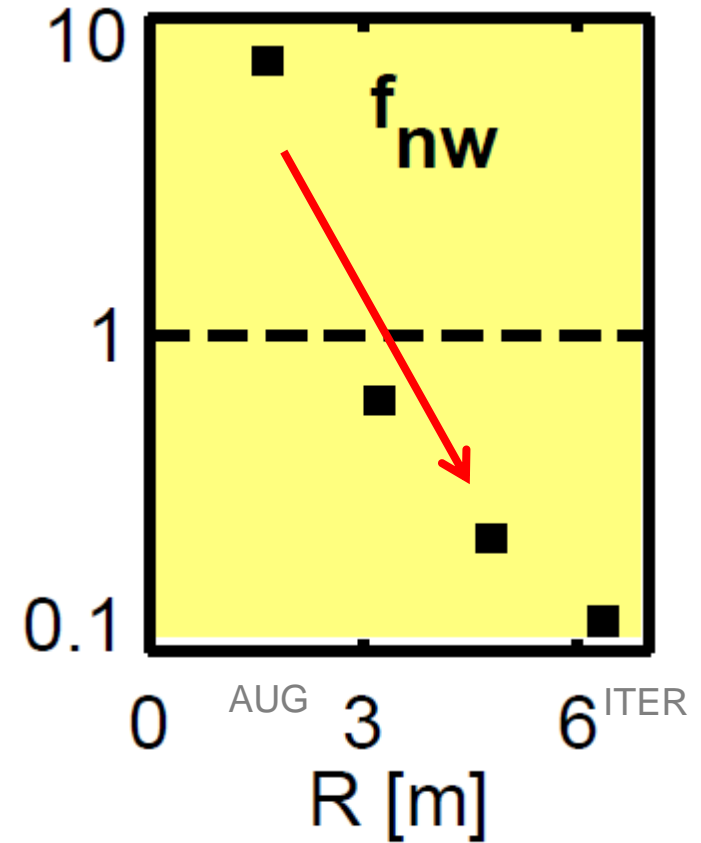
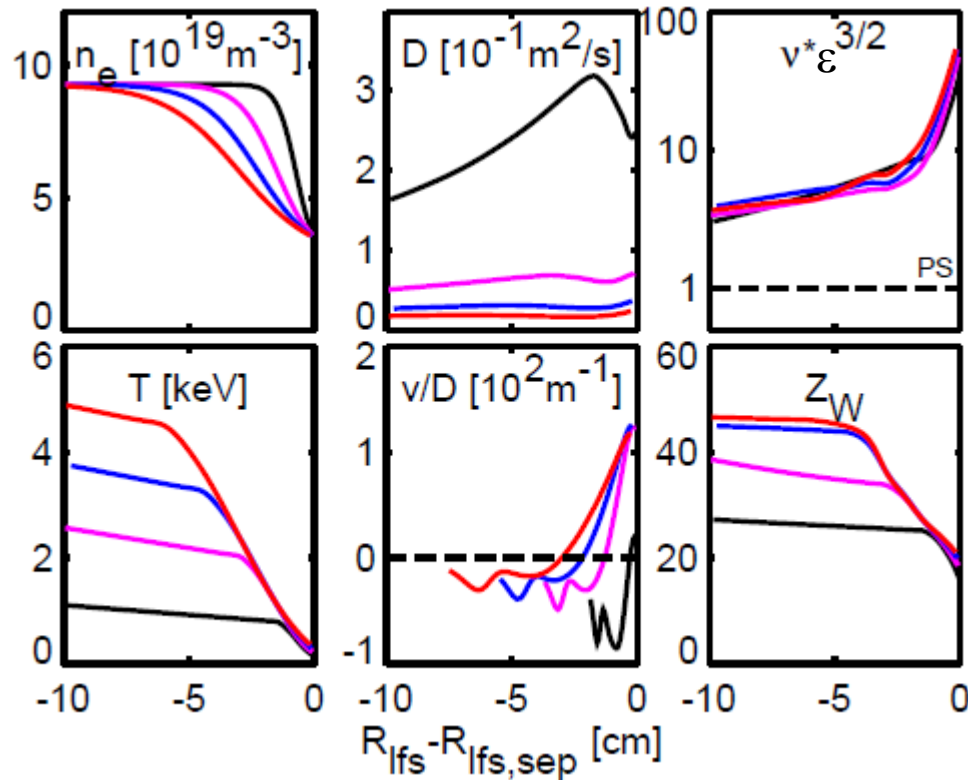
- favourable prospects for larger devices

Favourable tungsten behaviour expected in a large device



neoclassical W transport to predict pedestal scaling $n_{W,ped}/n_{W,sep}$

R. Dux, PSI 2016



higher temperature screening causes decrease of W density at pedestal top vs. separatrix

- successful ICRF antenna development (3-straps) for operation with tungsten PFCs
- massive W divertor performs well in high power – W released at crack edges not critical

despite challenges caused by high W concentrations with low gas input:

- fully non-inductive operation up to $I_p = 0.8$ MA
- ELM suppression with RMPs

achieved with the help of boronization in AUG

- favourable scaling of W transport for larger machines predicted

relative position of edge density and temperature profiles:

- important for confinement improvement by low-Z species
 - subject for future optimization with tailored pellet injection
-
- high divertor N enrichment in integrated divertor cooling scenario with pellets
→ pure core plasma with high divertor radiation and detachment

D. Aguiam², L. Aho-Mantila³, C. Angioni¹, N. Arden¹, R. Arredondo Parra¹, O. Asunta⁴, M. de Baar⁵, M. Balden¹, K. Behler¹, A. Bergmann¹, J. Bernardo², M. Bernert¹, M. Beurskens⁶, A. Biancalani¹, R. Bilato¹, G. Birkenmeier^{7,1}, V. Bobkov¹, A. Bock¹, A. Bogomolov⁵, T. Bolzonella³⁵, B. Bösowirth¹, C. Bottereau⁹, A. Bottino¹, H. van den Brand⁵, S. Brezinsek¹⁰, D. Brida^{1,7}, F. Brochard¹¹, C. Bruhn^{1,7}, J. Buchanan⁶, A. Buhler¹, A. Burckhart¹, D. Cambon-Silva¹, Y. Camenen⁹, P. Carvalho², G. Carrasco⁶, C. Cazzaniga⁸, M. Carr⁶, D. Carralero¹, L. Casali¹, C. Castaldo¹², M. Cavedon^{1,7}, C. Challis⁶, A. Chankin¹, I. Chapman⁶, F. Clairet⁷, I. Classen⁵, S. Coda¹³, R. Coelho², J.W. Coenen¹⁰, L. Colas⁹, G. Conway¹, S. Costea¹⁴, D.P. Coster¹, G. Croci¹², G. Cseh¹⁵, A. Czarnecka¹⁶, O. D'Arcangelo¹², C. Day¹⁷, R. Delogu¹², P. de Marne¹, S. Denk^{1,7}, P. Denner¹⁰, M. Dicon¹, R. D'Inca¹, A. Di Siena¹, D. Douai⁹, A. Drenik¹, R. Drube¹, M. Dunne¹, B.P. Duval¹³, R. Dux¹, T. Eich¹, S. Elgeti¹, K. Engelhardt¹, B. Erdős¹⁵, I. Erofeev¹, B. Esposito⁸, E. Fable¹, M. Faitsch¹, U. Fantz¹, H. Faugel¹, F. Felici¹⁸, S. Fietz¹, A. Figueredo⁵, R. Fischer¹, O. Ford¹, L. Frassinetti¹⁹, S. Freethy^{1,20}, M. Fröschle¹, G. Fuchert¹, J.C. Fuchs¹, H. Fünfgelder¹, K. Galazka¹⁶, J. Galdon-Quiroga²¹, A. Gallo⁹, Y. Gao¹⁰, S. Garavaglia¹², M. Garcia-Muñoz²¹, B. Geiger¹, C. Cianfarani¹², L. Giannone¹, E. Giovannozzi⁹, C. Gleason-González¹⁷, S. Glögler^{1,7}, M. Gobbin¹², T. Görler¹, T. Goodman¹³, G. Gorini¹², D. Gradic¹, A. Gräter¹, G. Granucci¹², H. Greuner¹, M. Griener^{1,7}, M. Groth⁴, A. Gude¹, S. Günter¹, L. Guimarães⁵, G. Haas¹, A.H. Hakola³, C. Ham⁶, T. Happel¹, J. Harrison⁶, D. Hatch²², V. Hauer¹⁷, T. Hayward¹, B. Heinemann¹, S. Heinzel²³, T. Hellsten¹⁹, S. Henderson⁶, P. Hennequin²⁴, A. Herrmann¹, E. Heyn²⁵, F. Hitzler¹, J. Hobirk¹, M. Hölzl¹, T. Höschen¹, J.H. Holm²⁶, C. Hopf¹, F. Hoppe¹, L. Horvath²⁷, A. Houben¹⁰, A. Huber⁷, V. Igochine¹, T. Ilkei¹⁴, I. Ivanova-Stanik¹⁶, W. Jacob¹, A.S. Jacobsen¹, J. Jacquot¹, F. Janky¹, A. Jardin⁹, F. Jaulmes⁵, F. Jenko²⁸, T. Jensen²⁶, E. Joffrin⁹, C. Käsemann¹, A. Kallenbach¹, S. Kálvin¹⁵, M. Kantor¹, A. Kappatou⁹, O. Kardaun¹, J. Karhunen⁴, S. Kasilov¹⁴, W. Kernbichler¹⁴, D. Kim¹³, S. Kimmig¹, A. Kirk⁶, H.-J. Klingenshirn¹, F. Koch¹, G. Kocsis¹⁵, A. Köhn¹, M. Kraus¹, K. Krieger¹, A. Krivska²⁹, A. Krämer-Flecken¹⁰, T. Kurki-Suonio⁴, B. Kurzan¹, K. Lackner¹, F. Lagner³⁰, P.T. Lang¹, P. Lauber¹, N. Lazányi²⁷, A. Lazaros³¹, A. Lebschy^{1,7}, L. Li¹⁰, M. Li¹, Y. Liang¹⁰, B. Lipschultz³², Y. Liu⁶, A. Lohs¹, N.C. Luhmann³³, T. Lunt¹, A. Lysoivan⁶, J. Madsen²⁶, H. Maier¹, O. Maj¹, J. Mailloux⁶, E. Maljaars¹⁷, P. Manas¹, A. Mancini¹², A. Manhard¹, M.-E. Manso², P. Mantica¹², M. Mantsinen³⁴, P. Manz^{7,1}, M. Maraschek¹, C. Martens¹, P. Martin³⁵, L. Marrelli¹², A. Maritsch¹², S. Mastrostefano¹², A. Mayer¹, M. Mayer¹, D. Mazon⁹, P.J. McCarthy³⁶, R. McDermott¹, G. Meisl¹, H. Meister¹, A. Medvedeva^{1,7}, P. Merkel¹, R. Merkel¹, A. Merle¹³, V. Mertens¹, D. Meshcheriakov¹, H. Meyer⁶, O. Meyer⁹, J. Miettunen⁴, D. Milanese⁸, F. Mink^{1,7}, A. Mlynck¹, F. Monaco¹, C. Moon¹, R. Nazikian³⁷, A. Nemes-Czopt¹⁵, G. Neu¹, R. Neu^{1,38}, A.H. Nielsen²⁶, S.K. Nielsen²⁶, V. Nikolaeva^{1,2,7}, M. Nocente¹², J.-M. Noterdaeme¹, S. Nowak¹², M. Oberkofler¹, M. Oberparleiter¹⁹, R. Ochoukov¹, T. Odstrcil^{1,7}, J. Olsen²⁶, F. Orain¹, F. Palermo¹, G. Papp¹, I. Paradela Perez⁴, G. Pautasso¹, F. Penzel¹, P. Petersson¹⁹, J. Pinzón^{1,7}, P. Piovesan³⁵, C. Piron³⁵, B. Plaum²⁵, B. Plöckl¹, V. Plyusnin², G. Pokol²⁷, E. Poli¹, L. Porte¹³, S. Potzel¹, D. Prisiazhniuk^{1,7}, T. Pütterich¹, M. Ramisch²⁵, C. Rapson¹, J. Rasmussen²⁶, G. Raupp¹, D. Réfy¹⁵, M. Reich¹, F. Reimold¹⁰, T. Ribeiro¹, R. Riedl¹, D. Rittich¹, G. Rocchi¹², M. Rodríguez-Ramos²¹, V. Rohde¹, A. Ross¹, M. Rott¹, M. Rubel¹⁹, D. Ryan⁶, F. Ryter¹, S. Saarela⁶, M. Salewski²⁶, A. Salmi³, L. Sanchis-Sanchez²¹, G. Santos², J. Santos², O. Sauter¹³, A. Scarabosio¹, G. Schall¹, K. Schmid¹, O. Schmitz³³, P.A. Schneider¹, M. Schneller¹, R. Schrittwieser³⁰, M. Schubert¹, T. Schwarz-Selinger¹, J. Schweinzer¹, B. Scott¹, T. Sehmer¹, M. Sertoli¹, A. Shabbir³⁹, A. Shalpegin¹¹, L. Shao⁴⁰, S. Sharapov⁶, M. Siccino¹, B. Sieglin¹, A. Sigalov¹, A. Silva², C. Silva², P. Simon^{1,11,25}, J. Simpson⁶, A.

Snicker¹, C. Sommariva⁹, C. Sozzi¹², M. Spolaore⁸, M. Stejner²⁶, J. Stober¹, F. Stobbe¹, U. Stroth^{1,7}, E. Strumberger¹, G. Suarez¹, K. Sugiyama¹, H.-J. Sun¹, W. Suttrop¹, T. Szepesi¹⁵, B. Tál¹⁵, T. Tala⁵, G. Tardini¹, M. Tardocchi¹², D. Terranova¹², W. Tierens¹, D. Told²⁸, O. Tudisco⁸, G. Trevisan³⁵, W. Treutterer¹, E. Trier¹, M. Tripsky²⁹, M. Valisa¹², M. Valovic⁶, B. Vanovac⁵, P. Varela², S. Varoutis¹⁷, G. Verdoolaege^{29,39}, D. Vezein¹, N. Vianello³⁵, J. Vicente², T. Vierle¹, E. Viezzer²¹, U. von Toussaint¹, D. Wagner¹, N. Wang⁹, X. Wang¹, M. Weidl¹, M. Weiland¹, A. E. White⁴¹, M. Willensdorfer¹, B. Wlinger¹, M. Wischmeier¹, R. Wolf¹, E. Wolfrum¹, L. Xiang⁴⁰, Q. Yang⁴⁰, Z. Yang¹, Q. Yu¹, R. Zagórski¹⁶, I. Zammuto¹, D. Zarzoso⁴², W. Zhang⁴⁰, M. van Zeeland²⁰, T. Zehetbauer¹, M. Zilker¹, S. Zoletnik¹⁵, H. Zohm¹.

¹IPP, Garching, Germany;

²Instituto de Plasmas e Fusão Nuclear, IST, Lisbon, Portugal;

³VTT, Espoo, Finland;

⁴Tekes, Aalto University, Helsinki, Finland;

⁵FOM-Institute DIFFER, TEC, Nieuwegein, The Netherlands;

⁶CCFE Fusion Association, Culham Science Centre, UK;

⁷Physik-Department E28, Technische Universität München, Garching;

⁸C.R.E. ENEA Frascati (Rome), Italy;

⁹CEA, IRFM, Cadarache, France;

¹⁰Forschungszentrum Jülich, Germany;

¹¹Institut Jean Lamour, CNRS, University of Nancy, France;

¹²ENEA, IFP, CNR, Milano, Italy;

¹³CRPP-EPFL, Lausanne, Switzerland;

¹⁴ÖAW, University of Innsbruck, Austria;

¹⁵Wigner Research Centre for Physics, Budapest, Hungary;

¹⁶Institute of Plasma Physics and Laser Microfusion, Hery 23, 01-497 Warsaw, Poland;

¹⁷KIT, Eggenstein-Leopoldshafen, Germany;

¹⁸Technische Universiteit Eindhoven, The Netherlands;

¹⁹VR, Stockholm, Sweden;

²⁰General Atomics, San Diego, CA, USA

²¹FAMN Department, Faculty of Physics, University of Seville, Seville, Spain;

²²Institute for Fusion Studies, University of Texas at Austin, Austin, TX 78712;

²³Max-Planck Computing and Data Facility, Garching;

²⁴LPP, CNRS, Ecole Polytechnique, Palaiseau, France;

²⁵IGVPT, Universität Stuttgart, Germany;

²⁶DTU, Kgs. Lyngby, Denmark;

²⁷Budapest University of Technology and Economics, Budapest, Hungary;

²⁸UCLA, University of California, LA, USA;

²⁹ERM/KMS, Brussels, Belgium;

³⁰ÖAW, IAP, TU Wien, Austria;

³¹Hellenic Republic, Athens, Greece;

³²University of York, York Plasma Institute, UK;

³³University of California, Davis, CA, USA;

³⁴ICREA-BSC, Barcelona, Spain;

³⁵Consorzio RFX, Padova, Italy;

³⁶DCU, University College, Cork, Ireland;

³⁷PPPL, Princeton, N.J., USA;

³⁸Technische Universität München, Garching;

³⁹Ghent University, Ghent, Belgium;

⁴⁰Chinese Academy of Sciences, Hefei, China;

⁴¹Plasma Science and Fusion Center, MIT, Cambridge, MA, USA;

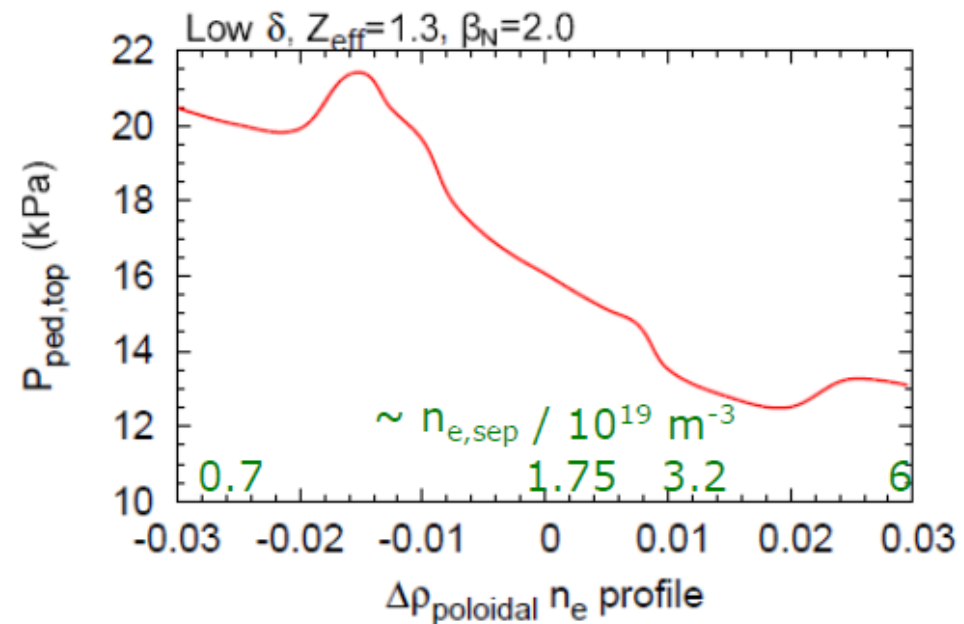
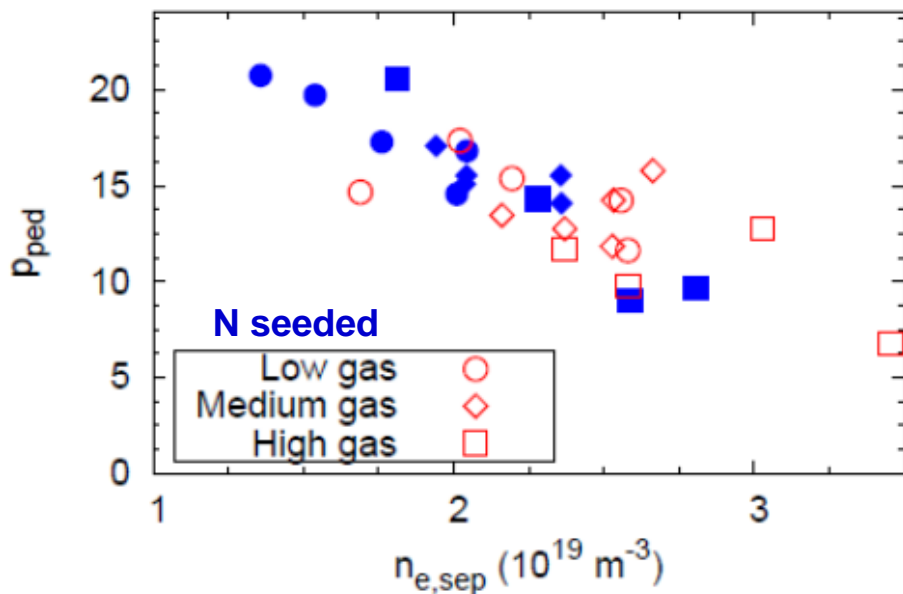
⁴²Aix-Marseille University, Marseille, France.

Reserve slide



Stability calculations confirm effect of n_e profile location on pedestal top pressure

- pedestal top pressure closely linked to density at separatrix
- further effects, like amplification of β increase by effect on shear



M. Dunne, EX/3-5, Wed

more on the AUG pedestal:

E. Viezzer, EX/P6-30, Thu

T. Pütterich, EX/P6-29, Thu